

Self-Assembly and -Cross-Linking Lamellar Films by Nanophase Separation with Solvent-Induced Anisotropic Structural Changes

Kohei Amada, Manabu Ishizaki, Masato Kurihara, and Jun Matsui*

Cite This: *ACS Omega* 2022, 7, 16778–16784

Read Online

ACCESS |



Metrics & More

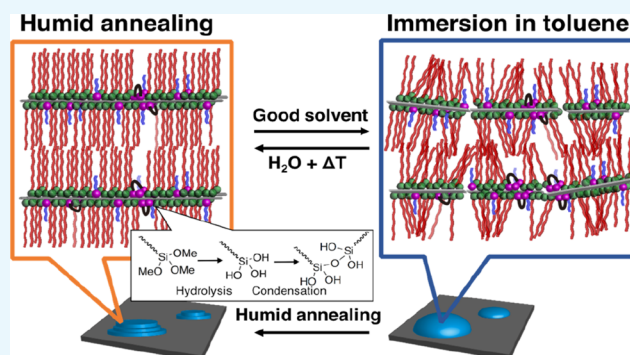


Article Recommendations



Supporting Information

ABSTRACT: In this study, we have prepared thermally and chemically stable lamellar polymer films via humid annealing. The amphiphilic polymer poly(*N*-dodecyl acrylamide-*stat*-3-(trimethoxysilyl)propyl acrylate) [p(DDA/TMSPA)] forms a self-assembled lamellar structure via annealing at 60 °C under 98% relative humidity (humid annealing) due to nanophase separation between the hydrophobic dodecyl side and main chains with the amide groups that contain adsorbed water. Moreover, a self-cross-linking reaction of TMSPA proceeds during the humid annealing. As a result, the lamellar films maintain their structure even when annealed above their glass-transition temperature. On the other hand, the films swell when immersed in toluene. The highly ordered lamellar structure collapses due to the swelling but can be re-established by subsequent humid annealing. A multilayer freestanding film can be exfoliated via sonication in toluene. The exfoliated multilayer films initially form a dome-shaped structure, which is converted to a plate-shaped structure upon humid annealing. In their entirety, these results reveal that the molecular-scale movement associated with the formation of the lamellar structure induces a macroscopic structural change. Consequently, p(DDA/TMSPA) can be considered as a new stimulus-responsive polymer.



INTRODUCTION

In general, polymeric materials with ordered structures exhibit improved functionality compared to those with randomly oriented conformations. For example, highly oriented polymer films exhibit mechanical strength that is by a factor of 7–15 higher than that of conventional films.^{1,2} Highly ordered polymer films also exhibit lower gas permeability (40–99% compared to amorphous films) due to the close packing of the polymer chains.^{3–5} Electron and ion conductivity can be improved by several orders of magnitude upon increasing the degree of orientation of the polymers.^{6–11} Most of these improvements have been achieved via the formation of highly oriented lamellar structures. Thus, the exploration of such highly ordered lamellar structures represents an effective method to create unique functional polymeric materials. So far, polymeric lamellar-structured materials have been prepared using crystalline polymers,^{12,13} liquid crystalline polymers,^{14–17} and block copolymers,^{18–20} while reports using amorphous homo- and copolymers remain scarce.^{21,22} In this context, we have discovered that a series of amorphous homo- and copolymers of alkyl acrylate and alkyl acrylamide form uniaxially oriented lamellar structures via annealing above their glass-transition temperatures (T_g) under humid conditions (humid annealing).^{23–28} During the humid annealing, water molecules adsorb on the hydrophilic amide and ester groups due to the highly humid conditions. As a result, segregation forces between the main chains that bear the

amide/ester groups with adsorbed water molecules and the alkyl side chains induce the formation of a lamellar structure via nanophase separation.^{23,25} These lamellar structures remain stable even after the water molecules are desorbed at a temperature below T_g , whereas they collapse to the initial amorphous state when annealed above T_g under dry conditions. This is because the segregation forces are insufficient due to the lack of water molecules in the hydrophilic region, therefore it returns to a thermodynamically stable random structure. Usually, such polymers are connected by relatively weak hydrophobic interactions and hydrogen bonds; therefore, the lamellar structure is unavoidably dissolved in common organic solvents. The notoriously unstable nature of poly(*N*-alkyl acrylamide) is an obstacle to the wide use of oriented films. Oriented films have applications, such as separation films, which require high thermal and chemical stability.

In this paper, we report a method to improve the thermal and mechanical stability of lamellar films of poly(*N*-dodecyl

Received: March 19, 2022

Accepted: April 26, 2022

Published: May 6, 2022



Table 1. Synthesis Condition of Copolymers and Their Composition, Molecular Weight, Polydispersity, and Thermal Properties

run	copolymer	molar ratio DDA/TMSPA in feed	molar ratio DDA/TMSPA in product	$M_n/10^4$	M_w/M_n	$T_g/^\circ\text{C}$	$T_M/^\circ\text{C}$	$T_{5d}/^\circ\text{C}$
1	p(DDA/TMSPA1) ^a	95:5	99:1	2.57	2.08	73.7	-35.2	335
2	p(DDA/TMSPA2) ^b	95:5	98:2	2.53	1.88	73.6	-37.2	304
3	p(DDA/TMSPA13) ^{a,c}	74:26	87:13	2.35	2.10	50.4	-35.6	349
4	p(DDA/TMSPA32) ^d	50:50	68:32	2.14	1.92	^e	-29.8	330

^aPolymerized at 60 °C for 12 h. ^bPolymerized at 65 °C for 12 h. ^cAnother p(DDA/TMSPA13) copolymer was synthesized (Table S1). ^dPolymerized at 60 °C for 24 h. ^eUnclear.

acrylamide [p(DDA)] by incorporating 3-(trimethoxysilyl)propyl acrylate (TMSPA) cross-linking groups using free radical copolymerization. The films of the copolymers were prepared using a spin-coating technique. We found that the copolymers with TMSPA contents of up to 13% form a uniaxially oriented lamellar structure upon humid annealing. Furthermore, the cross-linking of TMSPA also proceeds during the humid annealing. Therefore, these copolymers are promising materials for the creation of self-assembling and self-cross-linking lamellar films. Experimental evidence suggests that the lamellar structure of the copolymer is stably maintained even after eliminating the water molecules at annealing temperatures above T_g under vacuum. On the other hand, immersion of the cross-linked lamellar film in toluene resulted in partial structural collapse. The original lamellar film can be reformed by repeating the humid annealing. Interestingly, we found that the macroscale structure was also changed by the reformation of lamellae. In nature, *Mimosa pudica* folds its leaves in response to mechanical stimulation; this phenomenon is known as a seismonastic movement.²⁹ This macroscale (centimeter scale) motion is caused by the microscale contraction of cells via the drainage of water molecules. In the present film, a nanoscale structural change, that is, the formation of a lamellar structure via water absorption (influx of water), induces a microscale structural change in the film. Thus, such films can be considered as artificial micro-*M. pudica* mimics.

EXPERIMENTAL SECTION

Materials. DDA (TCI) was recrystallized from chloroform/hexane. 2,2'-Azobis(isobutyronitrile) (AIBN; Fujifilm Wako Pure Chemical Corp.) was recrystallized from ethanol. TMSPA (TCI), toluene (super dehydrated, Fujifilm Wako Pure Chemical Corp.), *n*-octyltrichlorosilane (Sigma-Aldrich), acetone (Nacalai Tesque Inc.), isopropyl alcohol (Nacalai Tesque Inc.), acetonitrile (Nacalai Tesque Inc.), chloroform (Kanto Chemical Co., Inc.), and tetrahydrofuran (THF; Kanto Chemical Co., Inc.) were used as received.

Synthesis of the Copolymers. Different feed ratios of DDA and TMSPA with 1 mol % of AIBN relative to the total monomer were dissolved in toluene at a concentration of 0.2 M. These solutions were degassed using three freeze-pump-thaw cycles, or the additions of toluene were conducted in an oxygen-free glovebox (GBJV065; Glovebox Japan Inc.). Then, the polymerizations were carried out at 60 or 65 °C for 12 or 24 h. After the copolymerization, the products were purified by three reprecipitations from chloroform into acetonitrile. The obtained polymers were vacuum dried at room temperature. The TMSPA contents were determined via ¹H NMR analysis of the integral ratio of the CH₃ groups of the dodecyl side chains and the OCH₃ groups of TMSPA (Table 1).

Preparation of Thin Films. A square silicon substrate (1 cm²) and a 1.3 cm × 3.5 cm quartz substrate were washed consecutively with acetone and isopropyl alcohol under sonication (ASU CLEANER, AS ONE Corp.) at 40 kHz for 20 min; this procedure was repeated twice. Subsequently, the substrate surface was treated with ultraviolet (UV)-O₃ irradiation for 30 min (PL16-110, SEN Lights Corp). The substrates were then immersed in chloroform with a few drops of *n*-trichlorooctylsilane, where they remained overnight to render their surfaces hydrophobic. Finally, the substrates were washed with chloroform and isopropyl alcohol under sonication at 40 kHz for 20 min. These hydrophobic substrates were stored in isopropyl alcohol and dried under the flow of N₂ prior to use.

The films were prepared via spin coating (MA-A100, Mikasa Co., Ltd.) of 5 wt % toluene solutions of the copolymers onto the hydrophobic substrates (1000 rpm for 5 s, then 1500 rpm for 60 s). Subsequently, the films were annealed under vacuum conditions (0.1 MPa) (ADP200; Yamato Scientific Co., Ltd.) at 80 °C for 1 h in order to remove any residual toluene. The substrates were then placed in a glass vessel with saturated K₂SO₄ aq, and the vessel was placed in an oven at 60 °C for humid annealing (Mini Oven MD-100; Yonezawa Corp.).

Peeling Off p(DDA/TMSPA) Films and Observation of Macroscopic Structural Changes. The humid-annealed films were immersed in toluene (10 mL) and sonicated at 40 kHz for 20 min to peel the p(DDA/TMSPA) films from the substrates. The film dispersion solutions were drop cast onto square silicon substrates (2 cm²) and dried under air.

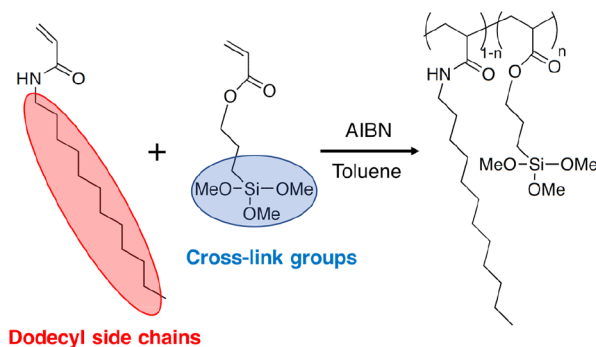
Measurements. NMR spectra were measured at room temperature using a JEOL ECA-500 spectrometer operating at 500 MHz. The number-average molecular weight (M_n) and polydispersity (M_w/M_n) of the polymers were measured via gel permeation chromatography (Shodex GPC-101, Showa Denko K.K.; polystyrene standards) at 40 °C in THF. The thermogravimetric analyses of the polymers were performed on a TGA-50 (Shimadzu Corp.) under a nitrogen flow (50 mL min⁻¹) at a heating rate of 10 °C min⁻¹ (temperature range: from room temperature to 800 °C). Differential scanning calorimetry (DSC) of polymers was performed on a DSC8231 (Rigaku Corp.) under a nitrogen flow (50 mL min⁻¹) at a heating and cooling rate of 10 °C min⁻¹. X-ray diffraction (XRD) measurements were conducted on a Rigaku SmartLab (Rigaku Corp.) with a Cu K α X-ray source ($\lambda = 0.1542$ nm) using a scintillation counter as the detector. The measurements were carried out in symmetrical reflection geometry (θ - 2θ method) and in-plane geometry at an incidence angle of 0.2° (2θ - χ method). The Fourier-transform infrared (FT-IR) spectra were obtained on an FT-IR spectrometer (Nicolet 6700; Thermo Fisher Scientific K. K.). The UV-visible (UV-vis) absorption spectra were recorded on a UV-vis-near-IR spectrophotometer (UV-3150, Shimadzu Corp.). The film

structure was analyzed via laser scanning microscopy (LM) (HYBRID L3; Lasertec Corp.) and atomic force microscopy (AFM) (XE-70; Park Systems Corp.). AFM measurements were carried out in dynamic mode using a silicon cantilever with a spring constant k of 1.7 N m^{-1} (OMCL-AC240TS-R3; Olympus Corp.).

RESULTS AND DISCUSSION

Synthesis of Copolymers. The copolymers of DDA and TMSPA [p(DDA/TMSPA)] were synthesized via free radical copolymerization (Scheme 1). Statistical copolymers result

Scheme 1. Synthesis of p(DDA/TMSPA) by Free radical Copolymerization Using AIBN as a Thermal Initiator at 60 or 65 °C for 12 or 24 h



from the simultaneous mixing and polymerization of two or more monomers.³⁰ The obtained copolymers were characterized using ^1H NMR and FT-IR spectroscopy. The ^1H NMR spectra show peaks related to the Si-OMe groups (3.6 ppm), dodecyl side chains (0.8–1.5 ppm), and polymer main chains (~ 2.4 ppm), together with the disappearance of the vinyl proton peaks (5.5–6.3 ppm) (Figures S1–S5).^{23,31} Moreover, the FT-IR spectra exhibit absorption bands associated with CH_3 asymmetric stretching (2955 cm^{-1}), CH_2 asymmetric stretching (2921 cm^{-1}), CH_2 symmetric stretching (2852 cm^{-1}), $\text{C}=\text{O}$ stretching (1644 cm^{-1} ; amide I), N–H bending (1540 cm^{-1} ; amide II), and Si–O– CH_3 asymmetric and symmetric stretching (1088 and 821 cm^{-1}) (Figure S6).^{23,31–33} In the case where the alkyl chain is in an all-trans conformation, the CH_2 asymmetric and symmetric stretching vibration appears at 2918 ± 1 and $2848 \pm 1 \text{ cm}^{-1}$, respectively. These peaks shifted to longer wavenumbers with an increase in gauche conformation.³⁴ The absorbance wavenumbers of CH_2 stretching vibrations indicate that the side chains are not all-trans conformation. The molecular weights of the p(DDA/TMSPA) copolymers were higher than 20,000 ($M_w/M_n = 1.88\text{--}2.10$) (Table 1). We have reported that $M_n > 6600$ is required to obtain highly oriented lamellar films.²⁸ Thus, the present molecular weight ($M_n > 20,000$) is sufficient to form a lamellar structure. The temperature at 5% weight loss (T_{5d}) was >300 °C for all the copolymers (Table 1 and Figure S7). The T_{5d} values of the copolymers are higher than those of pDDA,²³ suggesting that the introduction of inorganic components into the organic polymer increases its thermal stability. The DSC curves show two characteristic peaks in the scanning range. The endothermic peaks observed in the low-temperature region correspond to the melting of partially crystallized dodecyl groups,^{35–37} while the baseline shift observed at high temperatures originates from the T_g

(Table 1 and Figure S8). The T_g values decrease with increasing TMSPA content, therefore TMSPA is randomly incorporated into pDDA.³⁸ The DSC results suggest that p(DDA/TMSPA1), p(DDA/TMSPA2), and p(DDA/TMSPA13) are amorphous at room temperature.

Time Dependence of Hydrolysis and Condensation Reactions. The hydrolysis and condensation reactions of the p(DDA/TMSPA) copolymers were initially characterized using polymer powders. The condensation reactions of the copolymers with low TMSPA contents ($<2\%$) were hard to follow due to the small amount of cross-linking moieties. Therefore, we mainly used p(DDA/TMSPA13) to follow the condensation reaction. Figure 1 shows the FT-IR spectra of

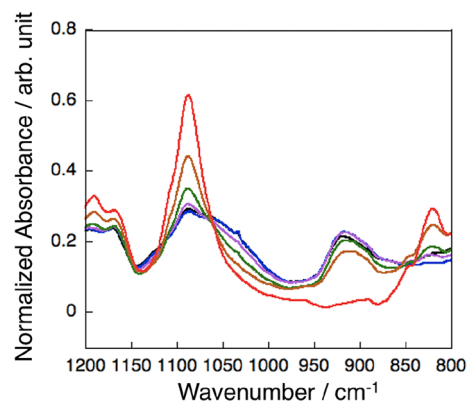


Figure 1. Normalized FT-IR spectra of p(DDA/TMSPA13) powder. Before humid annealing (red), and after humid annealing for 24 h (brown), 48 h (green), 72 h (purple), 96 h (blue), and 120 h (black). The spectra were normalized using the asymmetric stretching vibration of CH_2 .

p(DDA/TMSPA13) after varying exposure times to humid annealing. The FT-IR spectra clearly show a decrease in the Si-OMe peak (1088 cm^{-1}) and an increase in the Si-OH peak (916 cm^{-1}) with increasing humid annealing time. Similar trends were observed for p(DDA/TMSPA2) (Figure S9). The normalized Si-OMe peak intensities as a function of the humid annealing time suggest that the hydrolysis in the p(DDA/TMSPA) copolymers is almost complete after 48 h (Figure S10). Moreover, the formation of Si–O–Si bonds was confirmed by the appearance of an absorption at ca. 1030 cm^{-1} , which became clear after 72 h (Figure 1, purple spectrum). Thus, we concluded that the condensation reaction occurred mainly after the completion of the hydrolysis reaction.

Characterization of the Thin Films. Thin films of the copolymers were prepared via spin coating, and the structure of the films was studied using XRD measurements. Figure 2 shows the XRD patterns of the vacuum-annealed films. The broad diffractions at 2.4 nm^{-1} were attributed to the nanodomains of the dodecyl side chains (alkyl nanodomains).³⁵ The presence of the alkyl nanodomains indicated that the films were randomly oriented.^{35–37} The films were then humid annealed for 24 h (Figure 3). The XRD patterns of the humid-annealed films of p(DDA/TMSPA1) and p(DDA/TMSPA13) exhibit peaks with an integer ratio of 1:2:3, whereas the pattern of p(DDA/TMSPA2) was similar to that of the vacuum-annealed film. These results indicate that the copolymers with TMSPA content of up to 13% form ordered lamellar films via humid annealing. It should also be mentioned

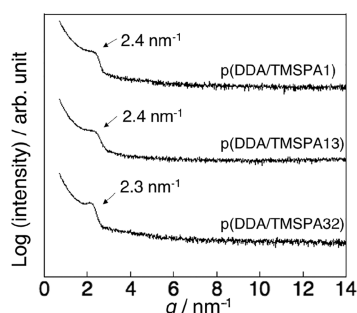


Figure 2. XRD patterns for p(DDA/TMSPA1) (top), p(DDA/TMSPA13) (center), and p(DDA/TMSPA32) (bottom) thin films annealed at 80 °C for 1 h under vacuum.

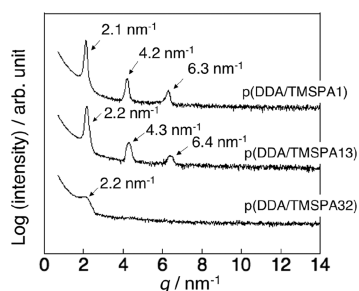


Figure 3. XRD patterns for p(DDA/TMSPA1) (top), p(DDA/TMSPA13) (center), and p(DDA/TMSPA32) (bottom) thin films annealed under humid conditions at 60 °C for 24 h.

here that films that were thermally annealed without humidity for 24 h showed only the diffraction characteristic for the alkyl nanodomains (Figure S11). As the FT-IR spectra revealed that the condensation reaction proceeds effectively after 72 h, we concluded that the self-cross-linking reaction mainly occurs after the formation of the lamellar structure during the humid annealing. The domain spacing of p(DDA/TMSPA1) and p(DDA/TMSPA13) was estimated to be 3.0 and 2.9 nm from the peaks at 2.1 and 2.2 nm⁻¹, respectively. The values were smaller than that of the pDDA homopolymer ($d = 3.25$ nm)²³ because TMSPA groups inhibit the packing of the alkyl side chains. Moreover, the diffraction at 14 nm⁻¹, which was attributed to hexagonal-like packing of the dodecyl side chains, was only observed in the in-plane direction (Figure S12).^{35–37}

The repeating units were aligned with the short-axis direction of the packing. The XRD patterns thus indicate the formation of an uniaxially oriented lamellar structure, wherein the polymer main chains form the lamellar plane with the dodecyl side chains oriented perpendicular to the lamellar plane (Figure 4).

Stability of Self-Cross-Linked Lamellar Films toward Heat and Organic Solvents. Thin films of p(DDA/TMSPA2) and p(DDA/TMSPA13) were humidly annealed for 96 h and their stability was examined. To study their thermal stability, the lamellar-structured films were annealed under vacuum at 80 °C for 24 h. The XRD patterns of the thermally annealed films exhibited integer ratio peaks in the out-of-plane direction and an amorphous halo corresponding to the dodecyl side chains with hexagonal-like packing in the in-plane direction (Figure 5). We have previously reported that, under the same thermal annealing conditions, a lamellar film of the homopolymer pDDA collapsed to become amorphous.²³ Thus, the XRD results indicate that the thermal

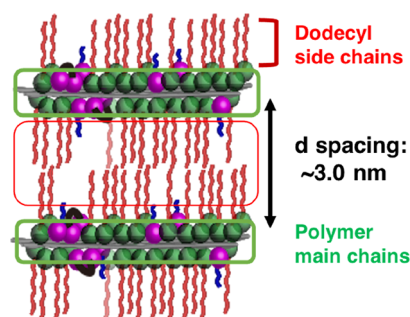


Figure 4. Schematic image of the lamellar structure of thin films of p(DDA/TMSPA). Red, green, purple, and blue represent dodecyl side chains, amide, ester, and 3-(trimethoxysilyl)propyl groups, respectively.

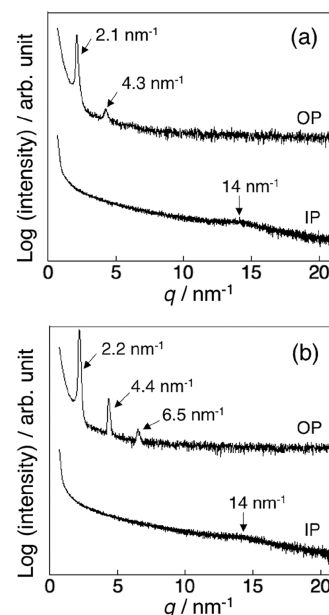


Figure 5. XRD patterns of the thin films of (a) p(DDA/TMSPA2) and (b) p(DDA/TMSPA13) after exposure to humid annealing conditions at 60 °C for 96 h, followed by annealing at 80 °C for 24 h under vacuum. In each figure, the top and bottom patterns are the patterns measured in the out-of-plane and in-plane directions, respectively.

stability of the lamellar films is increased by the formation of Si–O–Si bonds.

Next, we evaluated the solvent resistance of the lamellar films by immersing the humid-annealed thin films in the good solvent toluene for 24 h at room temperature, before measuring their UV–vis and FT-IR spectra and XRD patterns. The UV–vis spectra of the humid-annealed films exhibit an absorption at around 190 nm, which was attributed to the amide groups.³⁹ After immersion in toluene, the absorption almost disappeared from the spectrum of the p(DDA/TMSPA2) film, whereas only a 6% absorption decrease was observed for the p(DDA/TMSPA13) film (Figure S13). Similar trends were observed in the FT-IR spectra. In the FT-IR spectrum of p(DDA/TMSPA2), the peaks in the C–H stretching region (2800–3000 cm⁻¹) and the N–H stretching vibration (3307 cm⁻¹) almost disappeared after immersion in toluene, while they remained in the spectrum of the p(DDA/TMSPA13) film (Figure S14). The UV–vis and FT-IR spectra indicate that at least 13% TMSPA is required to prevent the

films from dissolving in a good solvent. It should be mentioned that copolymers with a low TMSPA content did not fully dissolve; part of the film peeled off in the form of nanosheets (vide infra). The XRD pattern of the toluene-immersed p(DDA/TMSPA13) film exhibited only a sharp first-order peak at 2.3 nm^{-1} (Figure 6a), which is due to the swelling of

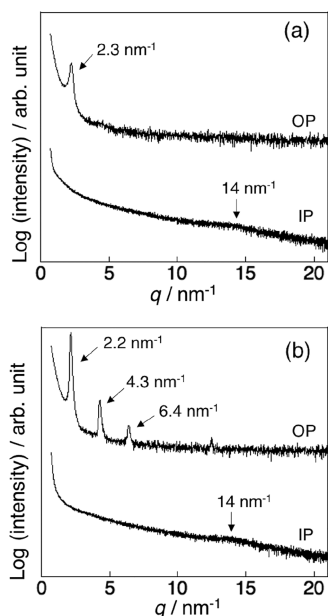


Figure 6. XRD patterns of a humid-annealed thin film of p(DDA/TMSPA13) (a) after immersion in toluene and (b) after humid annealing of the toluene-immersed film. In each figure, the top and bottom patterns are the patterns measured in the out-of-plane and in-plane directions, respectively.

the lamellar film in toluene, which disrupts the layer structure. We assumed that the uniform lamellar structure could potentially be recovered after repeating the humid annealing. Therefore, we exposed the toluene-immersed film for 24 h to humid annealing conditions and characterized the film structure using XRD. The XRD pattern of the film after re-annealing exhibits strong Bragg peaks of up to the third order, which indicates that the uniform lamellar structure was reformed (Figure 6b). Thus, the partial disruption of the lamellar structure by swelling and the reformation of the highly ordered structure by humid annealing are reversible (Figure 7). It should also be mentioned here that the lamellar film was not reformed by annealing without humidity (Figure S15).

Exfoliation of Lamellar Sheets. We discovered that multilayer sheets of the copolymer could be exfoliated by sonication in toluene. To peel off the film, we first immersed

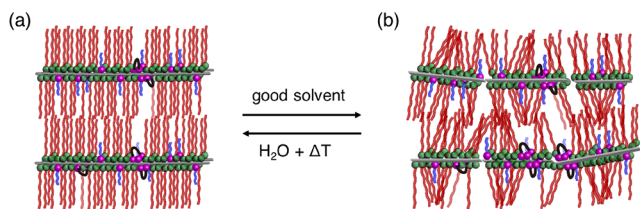


Figure 7. Schematic images of the reversible change in the structure between the thin films of (a) humid-annealed and (b) toluene-immersed p(DDA/TMSPA).

the Si substrate with the humid-annealed film in toluene and subjected it to sonication for 20 min. The toluene solution was then dropped on the Si substrate, and the surface of the film was observed using LM and AFM. As discussed above, the layered lamellar structure collapsed upon immersion in toluene and was subsequently reformed by repeating the humid annealing. We surmised that this molecular-scale orientational change induced the macroscopic structural change. Thus, we studied the structural change of a relatively thick self-standing film. Figure 8 shows the LM and AFM images of a self-standing p(DDA/TMSPA1) film before and after humid annealing. All the images are of the same film, as can be confirmed from the protruding structures indicated by the green arrows. The self-standing film, with a size of $40 \mu\text{m}^2$, exhibited a dome-like shape with a height of $\sim 110 \text{ nm}$. However, the “roof” became flat and its height decreased to $\sim 60 \text{ nm}$ after humid annealing. We concluded that this structural change was induced by the formation of the uniformly oriented lamellar structure. The lamellar structure of the as-exfoliated films is disrupted by toluene, and the polymer tends to form a round shape to reduce the surface area. Humid annealing of the as-exfoliated film induced the formation of a lamellar structure; thus, the structure became angular and the surface became flat. A macroscopic structural change was also observed in a self-standing p(DDA/TMSPA13) film with a size of $20 \mu\text{m}^2$ (Figure S16). The dome-like shape of the self-standing p(DDA/TMSPA13) film shrank and its “roof” became flat after humid annealing. As indicated in the introduction section and our previous results,^{23–28} the formation of a lamellar structure in the p(DDA/TMSPA) films was induced by the adsorption of water on the hydrophilic amide groups. In general, polymers swell isotropically due to solvent adsorption. In contrast, the present copolymers shrink and form an anisotropic angular structure upon the adsorption of water. These macroscopic anisotropic structural changes are induced by the formation of a nanoscale lamellar structure of polymer chains due to the adsorption of water. The mechanism of this structural change resembles the seismonastic movement of *M. pudica*; thus, these p(DDA/TMSPA) copolymers can be thought of as artificial micro-*M. pudica* mimics.

CONCLUSIONS

Thermally and chemically stable amorphous lamellar films were prepared by the humid annealing of thin films of p(DDA/TMSPA). Copolymers with TMSPA content of up to 13% formed highly oriented lamellar films upon humid annealing, which also induced the cross-linking reaction of the TMSPA groups. Completing the cross-linking reaction required a humid annealing time three times longer than that required for the formation of the lamellar structure. Therefore, we concluded that the cross-linking reaction occurred predominantly after the formation of the lamellar structure. Cross-linking also improved the thermal stability of the films; that is, the lamellar structure is maintained even after thermal annealing above the glass-transition temperature (T_g). Immersion of such cross-linked films in toluene results in swelling and hence partial collapse of the lamellar structure, albeit that the highly oriented lamellar structure can be recovered by humid annealing. In summary, we have demonstrated that macroscopic structural changes can be induced in multilayer p(DDA/TMSPA) sheets via humid

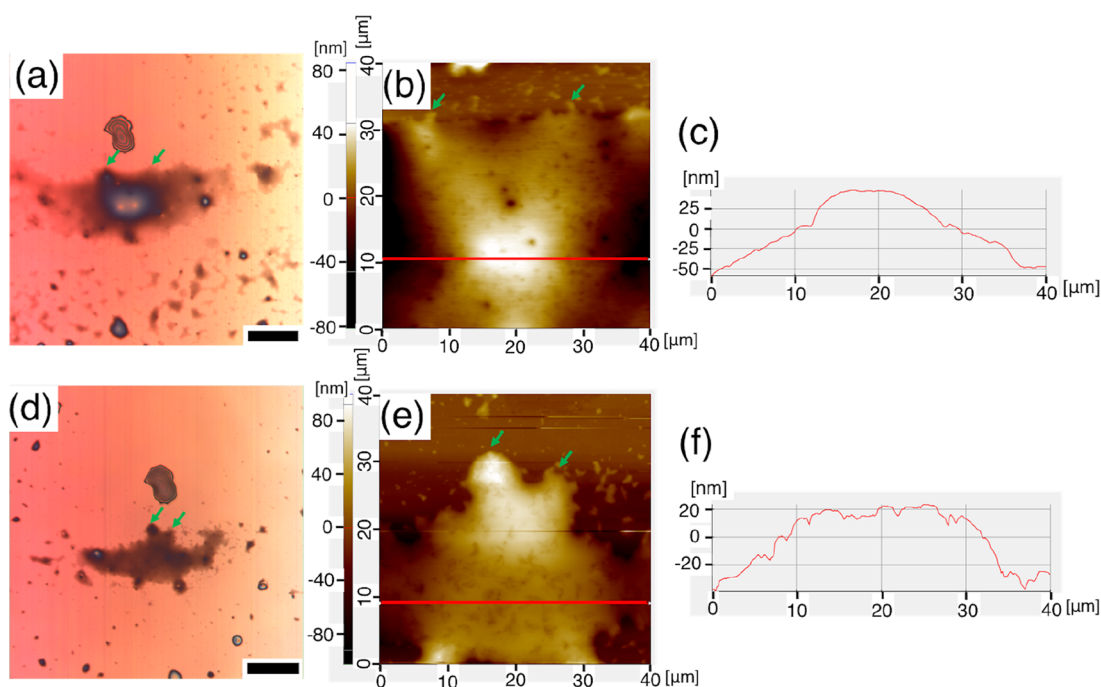


Figure 8. LM images and AFM topological images of p(DDA/TMSPA1) films before (a,b) and after (d,e) humid annealing; (c,f) represent the line profiles for (b,e), respectively. (Scale bar: 25 μm).

annealing. Thus, these copolymers can be considered as a new stimulus-responsive material that mimics *M. pudica*.

■ ASSOCIATED CONTENT

Supporting Information

The Supporting Information is available free of charge at <https://pubs.acs.org/doi/10.1021/acsomega.2c01675>.

¹H NMR, FT-IR, and UV–vis spectra of the (co)-polymers and XRD patterns and AFM and LM images of the (co)polymer films (PDF)

■ AUTHOR INFORMATION

Corresponding Author

Jun Matsui – Faculty of Science, Yamagata University, Yamagata 990-8560, Japan; orcid.org/0000-0003-4767-4507; Email: jun_m@sci.kj.yamagata-u.ac.jp

Authors

Kohei Amada – Graduate School of Science and Engineering, Yamagata University, Yamagata 990-8560, Japan

Manabu Ishizaki – Faculty of Science, Yamagata University, Yamagata 990-8560, Japan; orcid.org/0000-0003-0522-1825

Masato Kurihara – Faculty of Science, Yamagata University, Yamagata 990-8560, Japan; orcid.org/0000-0002-5215-6264

Complete contact information is available at: <https://pubs.acs.org/doi/10.1021/acsomega.2c01675>

Notes

The authors declare no competing financial interest.

■ ACKNOWLEDGMENTS

This work was supported by the KAKENHI grant 18H02026 from the Japan Society for the Promotion of Science (JSPS),

JST, CREST Grant Number JPMJCR21B5, the CASIO SCIENCE PROMOTION FOUNDATION, the Fuji Seal Foundation, 2021 Yamagata University—Center of Excellence (Collaboration) [YU-COE(C)] program, “Yamagata University Carbon Neutral Research Center (YUCaN)”, and the Research Program “Dynamic Alliance for Open Innovation Bridging Human, Environment and Materials” within the “Network Joint Research Center for Materials and Devices”.

■ REFERENCES

- (1) Lu, H.-F.; Wang, M.; Chen, X.-M.; Lin, B.-P.; Yang, H. Interpenetrating Liquid-Crystal Polyurethane/Polyacrylate Elastomer with Ultrastrong Mechanical Property. *J. Am. Chem. Soc.* **2019**, *141*, 14364–14369.
- (2) Xi, P.; Quan, F.; Yao, J.; Xia, Y.; Fang, K.; Jiang, Y. Strategy to Fabricate a Strong and Supertough Bio-Inspired Fiber with Organic–Inorganic Networks in a Green and Scalable Way. *ACS Nano* **2021**, *15*, 16478–16487.
- (3) Miyashita, T.; Konno, M.; Matsuda, M.; Saito, S. Oxygen Enrichment by a Langmuir-Blodgett Film of Poly(N-dodecylacrylamide) on Porous Aluminum Oxide. *Macromolecules* **1990**, *23*, 3531–3533.
- (4) Messin, T.; Follain, N.; Guinault, A.; Sollogoub, C.; Gaucher, V.; Delpouve, N.; Marais, S. Structure and Barrier Properties of Multilayered Biodegradable PLA/PBSA Films: Confinement Effect via Forced Assembly Coextrusion. *ACS Appl. Mater. Interfaces* **2017**, *9*, 29101–29112.
- (5) Kong, P.; Deng, J.; Du, Z.; Zou, W.; Zhang, C. Construction of Lamellar Morphology by Side-Chain Crystalline Comb-like Polymers for Gas Barrier. *Polym. Adv. Technol.* **2022**, *33*, 280–289.
- (6) Han, M. J.; Lee, D.-W.; Lee, E. K.; Kim, J.-Y.; Jung, J. Y.; Kang, H.; Ahn, H.; Shin, T. J.; Yoon, D. K.; Park, J.-I. Molecular Orientation Control of Liquid Crystal Organic Semiconductor for High-Performance Organic Field-Effect Transistors. *ACS Appl. Mater. Interfaces* **2021**, *13*, 11125–11133.
- (7) Han, M. J.; McBride, M.; Risteen, B.; Zhang, G.; Khau, B. V.; Reichmanis, E.; Yoon, D. K. Highly Oriented and Ordered Water-Soluble Semiconducting Polymers in a DNA Matrix. *Chem. Mater.* **2020**, *32*, 688–696.

- (8) Nagao, Y.; Matsui, J.; Abe, T.; Hiramatsu, H.; Yamamoto, H.; Miyashita, T.; Sata, N.; Yugami, H. Enhancement of Proton Transport in an Oriented Polypeptide Thin Film. *Langmuir* **2013**, *29*, 6798–6804.
- (9) Sato, T.; Hayasaka, Y.; Mitsuishi, M.; Miyashita, T.; Nagano, S.; Matsui, J. High Proton Conductivity in the Molecular Interlayer of a Polymer Nanosheet Multilayer Film. *Langmuir* **2015**, *31*, 5174–5180.
- (10) Yoshio, M.; Kagata, T.; Hoshino, K.; Mukai, T.; Ohno, H.; Kato, T. One-Dimensional Ion-Conductive Polymer Films: Alignment and Fixation of Ionic Channels Formed by Self-Organization of Polymerizable Columnar Liquid Crystals. *J. Am. Chem. Soc.* **2006**, *128*, 5570–5577.
- (11) Kato, T.; Yoshio, M.; Ichikawa, T.; Soberats, B.; Ohno, H.; Funahashi, M. Transport of Ions and Electrons in Nanostructured Liquid Crystals. *Nat. Rev. Mater.* **2017**, *2*, 17001.
- (12) Shen, J.; Zhou, Y.; Lu, Y.; Wang, B.; Shen, C.; Chen, J.; Zhang, B. Later Stage Melting of Isotactic Polypropylene. *Macromolecules* **2020**, *53*, 2136–2144.
- (13) Ito, A.; Hioki, K.; Kono, K.; Hiejima, Y.; Nitta, K.-h. Effects of Liquid Paraffin on Dynamic Mechanical Properties of Linear High-Density Polyethylene. *Macromolecules* **2020**, *53*, 8459–8466.
- (14) Imanishi, R.; Nagashima, Y.; Takishima, K.; Hara, M.; Nagano, S.; Seki, T. Induction of Highly Ordered Smectic Phases in Side Chain Liquid Crystalline Polymers by Means of Random Copolymerization. *Macromolecules* **2020**, *53*, 1942–1949.
- (15) Orodepo, G. O.; Gowd, E. B.; Ramakrishnan, S. Periodically Spaced Side-Chain Liquid Crystalline Polymers. *Macromolecules* **2020**, *53*, 8775–8786.
- (16) Lv, J.-a.; Liu, Y.; Wei, J.; Chen, E.; Qin, L.; Yu, Y. Photocontrol of Fluid Slugs in Liquid Crystal Polymer Microactuators. *Nature* **2016**, *537*, 179–184.
- (17) Zhao, N.; Botton, G. A.; Zhu, S.; Duft, A.; Ong, B. S.; Wu, Y.; Liu, P. Microscopic Studies on Liquid Crystal Poly(3,3'-dialkylquaterthiophene) Semiconductors. *Macromolecules* **2004**, *37*, 8307–8312.
- (18) Kamata, Y.; Parnell, A. J.; Gutfreund, P.; Skoda, M. W. A.; Dennison, A. J. C.; Barker, R.; Mai, S.; Howse, J. R.; Ryan, A. J.; Torikai, N.; Kawaguchi, M.; Jones, R. A. L. Hydration and Ordering of Lamellar Block Copolymer Films under Controlled Water Vapor. *Macromolecules* **2014**, *47*, 8682–8690.
- (19) Cummins, C.; Ghoshal, T.; Holmes, J. D.; Morris, M. A. Strategies for Inorganic Incorporation Using Neat Block Copolymer Thin Films for Etch Mask Function and Nanotechnological Application. *Adv. Mater.* **2016**, *28*, 5586–5618.
- (20) Kennemur, J. G.; Hillmyer, M. A.; Bates, F. S. Synthesis, Thermodynamics, and Dynamics of Poly(4-tert-butylstyrene-*b*-methyl methacrylate). *Macromolecules* **2012**, *45*, 7228–7236.
- (21) Ikami, T.; Watanabe, Y.; Ogawa, H.; Takenaka, M.; Yamada, N. L.; Ouchi, M.; Aoki, H.; Terashima, T. Multilayered Lamellar Materials and Thin Films by Instant Self-Assembly of Amphiphilic Random Copolymers. *ACS Macro Lett.* **2021**, *10*, 1524–1528.
- (22) Ikami, T.; Kimura, Y.; Takenaka, M.; Ouchi, M.; Terashima, T. Design Guide of Amphiphilic Crystalline Random Copolymers for Sub-10 nm Microphase Separation. *Polym. Chem.* **2021**, *12*, 501–510.
- (23) Hashimoto, Y.; Sato, T.; Goto, R.; Nagao, Y.; Mitsuishi, M.; Nagano, S.; Matsui, J. In-Plane Oriented Highly Ordered Lamellar Structure Formation of Poly(N-Dodecylacrylamide) Induced by Humid Annealing. *RSC Adv.* **2017**, *7*, 6631–6635.
- (24) Matsunaga, K.; Kukai, W.; Ishizaki, M.; Kurihara, M.; Yamamoto, S.; Mitsuishi, M.; Yabu, H.; Nagano, S.; Matsui, J. Formation of Perpendicularly Aligned Sub-10 nm Nanocylinders in Poly(N-Dodecylacrylamide-*b*-Ethylene Glycol) Block Copolymer Films by Hierarchical Phase Separation. *Macromolecules* **2020**, *53*, 9601–9610.
- (25) Ebata, K.; Hashimoto, Y.; Yamamoto, S.; Mitsuishi, M.; Nagano, S.; Matsui, J. Nanophase Separation of Poly(N-Alkyl Acrylamides): The Dependence of the Formation of Lamellar Structures on Their Alkyl Side Chains. *Macromolecules* **2019**, *52*, 9773–9780.
- (26) Ebata, K.; Togashi, T.; Yamamoto, S.; Mitsuishi, M.; Matsui, J. Self Formed Anisotropic Proton Conductive Polymer Film by Nanophase Separation. *J. Electrochem. Soc.* **2019**, *166*, B3218–B3222.
- (27) Matsunaga, K.; Tanaka, K.; Matsui, J. Highly Ordered Lamellar Formation in Dodecylacrylate Copolymer by Humid Annealing. *Chem. Lett.* **2018**, *47*, 500–502.
- (28) Ebata, K.; Hashimoto, Y.; Ebara, K.; Tsukamoto, M.; Yamamoto, S.; Mitsuishi, M.; Nagano, S.; Matsui, J. Molecular-weight dependence of the formation of highly ordered lamellar structures in poly(N-dodecyl acrylamide) by humid annealing. *Polym. Chem.* **2019**, *10*, 835–842.
- (29) Hagihara, T.; Toyota, M. Mechanical Signaling in the Sensitive Plant *Mimosa pudica* L. *Plants* **2020**, *9*, 587.
- (30) Jenkins, A. D.; Loening, K. L. *Comprehensive Polymer Science and Supplements*; Pergamon, 1989.
- (31) Maçon, A. L. B.; Greasley, S. L.; Becer, C. R.; Jones, J. R. RAFT Polymerization of N-[3-(Trimethoxysilyl)-propyl]acrylamide and Its Versatile Use in Silica Hybrid Materials. *Macromol. Rapid Commun.* **2015**, *36*, 2060–2064.
- (32) Maeda, Y.; Higuchi, T.; Ikeda, I. Change in Hydration State during the Coil-Globule Transition of Aqueous Solutions of Poly(N-isopropylacrylamide) as Evidenced by FTIR Spectroscopy. *Langmuir* **2000**, *16*, 7503–7509.
- (33) Hooshmand, T.; van Noort, R.; Keshvad, A. Storage Effect of a Pre-Activated Silane on the Resin to Ceramic Bond. *Dent. Mater.* **2004**, *20*, 635–642.
- (34) Zhang, Z.; Verma, A. L.; Yoneyama, M.; Nakashima, K.; Iriyama, K.; Ozaki, Y. Molecular Orientation and Aggregation in Langmuir-Blodgett Films of 5-(4-N-Octadecylpyridyl)-10,15,20-trip-Tolyporphyrin Studied by Ultraviolet-Visible and Infrared Spectroscopies. *Langmuir* **1997**, *13*, 4422–4427.
- (35) Beiner, M.; Huth, H. Nanophase Separation and Hindered Glass Transition in Side-Chain Polymers. *Nat. Mater.* **2003**, *2*, 595–599.
- (36) Hiller, S.; Pascui, O.; Budde, H.; Kabisch, O.; Reichert, D.; Beiner, M. Nanophase Separation in Side Chain Polymers: New Evidence from Structure and Dynamics. *New J. Phys.* **2004**, *6*, 10.
- (37) McCreight, K. W.; Ge, J. J.; Guo, M.; Mann, I.; Li, F.; Shen, Z.; Jin, X.; Harris, F. W.; Cheng, S. Z. D. Phase Structures and Transition Behaviors in Polymers Containing Rigid Rodlike Backbones with Flexible Side Chains. V. Methylene Side-Chain Effects on Structure and Molecular Motion in a Series of Polyimides. *J. Polym. Sci., Part B: Polym. Phys.* **1999**, *37*, 1633–1646.
- (38) Huang, C.-C.; Du, M.-X.; Zhang, B.-Q.; Liu, C.-Y. Glass Transition Temperatures of Copolymers: Molecular Origins of Deviation from the Linear Relation. *Macromolecules* **2022**, *55*, 3189–3200.
- (39) Zhu, H.; Mitsuishi, M.; Miyashita, T. Facile Preparation of Highly Oriented Poly(vinylidene fluoride) Langmuir–Blodgett Nanofilms Assisted by Amphiphilic Polymer Nanosheets. *Macromolecules* **2012**, *45*, 9076–9084.